10740–10750 *Nucleic Acids Research, 2017, Vol. 45, No. 18* *Published online 16 August 2017*
doi: 10.1093/nar/gkx726

Allosteric regulation of Csx1, a type IIIB-associated CARF domain ribonuclease by RNAs carrying a tetraadenylate tail

Wenyuan Han[1], Saifu Pan[2], Blanca López-Méndez[3], Guillermo Montoya[4] and Qunxin She[1,2,*]

[1]Archaea Center, Department of Biology, University of Copenhagen, Ole Maaløes Vej 5, Copenhagen Biocenter, DK-2200 Copenhagen N, Denmark, [2]State Key Laboratory of Agricultural Microbiology and College of Life Science and Technology, Huazhong Agricultural University, 430070 Wuhan, China, [3]Protein Structure & Function Programme, Protein Production and Characterization Platform, Faculty of Health and Medical Sciences, University of Copenhagen, Blegdamsvej 3B, DK-2200 Copenhagen, Denmark and [4]Macromolecular Crystallography Group, Novo Nordisk Foundation Center for Protein Research, Faculty of Health and Medical Sciences, University of Copenhagen, Blegdamsvej 3B, DK-2200 Copenhagen, Denmark

Received July 10, 2017; Revised August 03, 2017; Editorial Decision August 04, 2017; Accepted August 08, 2017

ABSTRACT

CRISPR–Cas systems protect prokaryotes against invading viruses and plasmids. The system is associated with a large number of Cas accessory proteins among which many contain a CARF (CRISPR-associated Rossmann fold) domain implicated in ligand binding and a HEPN (higher eukaryotes and prokaryotes nucleotide-binding) nuclease domain. Here, such a dual domain protein, i.e. the *Sulfolobus islandicus* Csx1 (SisCsx1) was characterized. The enzyme exhibited metal-independent single-strand specific ribonuclease activity. In fact, SisCsx1 showed a basal RNase activity in the absence of ligand; upon the binding of an RNA ligand carrying four continuous adenosines at the 3′-end (3′-tetra-rA), the activated SisCsx1 degraded RNA substrate with a much higher turnover rate. Amino acid substitution mutants of SisCsx1 were obtained, and characterization of these mutant proteins showed that the CARF domain of the enzyme is responsible for binding to 3′-tetra-rA and the ligand binding strongly activates RNA cleavage by the HEPN domain. Since RNA polyadenylation is an important step in RNA decay in prokaryotes, and poly(A) RNAs can activate CARF domain proteins, the poly(A) RNA may function as an important signal in the cellular responses to viral infection and environmental stimuli, leading to degradation of both viral and host transcripts and eventually to cell dormancy or cell death.

INTRODUCTION

Clustered regularly interspaced short palindromic repeats (CRISPR) loci and CRISPR-associated (Cas) proteins is the inheritable and adaptive immune system that protects bacteria and archaea from invasion by viruses and plasmids (1,2). The system is able to acquire a short fragment from foreign genetic elements and insert into the CRISPR loci as a new spacer. Then transcription of CRISPR loci and processing of the transcripts generate CRISPR RNA (crRNA) based on each spacer. Finally, crRNA guides Cas proteins (a protein complex or a single protein) to recognize and destroy invading DNA and/or RNA. Therefore, there are three basic steps in the CRISPR immunity: new spacer acquisition, biogenesis of crRNA and interference of invading nucleic acid (1–5).

In addition, CRISPR–Cas systems are usually associated with genes that appear to be not directly involved in the three steps (5). The proteins encoded by such genes, usually termed non-core Cas accessory proteins, are still poorly characterized. The most widespread group of accessory proteins contain a predicted nucleotide-binding domain with a Rossmann-like fold and are denoted CARF (CRISPR-associated Rossmann fold) domain proteins (6). In the proteins belonging to this group, the CARF domain is usually fused to another effector domain, such as a winged helix-turn-helix (wHTH) DNA binding domain, a DNase domain of the restriction endonuclease or an RNase domain belonging to either RelE or HEPN (higher eukaryotes and prokaryotes nucleotide-binding) families (6–9). Since Rossmann folds are known to function in ligand binding, it is predicted that the CARF domain could have an allosteric regulatory function upon binding to a ligand molecule. In the crystal structures solved for a few CARF domain proteins, a ligand-binding site is predicted in

*To whom correspondence should be addressed. Tel: +45 3532 2013; Fax: +45 3532 2128; Email: qunxin@bio.ku.dk

the CARF domain containing several amino acids residues (10–12), and furthermore, a co-crystal structure has been solved for the *Archaeoglobus fulgidus* Csx3, a single domain CARF protein and a tetranucleotide that binds to the protein (12).

Within the CARF group, Csm6 and Csx1 proteins are encoded by the genes evolutionarily linked with type III CRISPR–Cas systems (4,13), the only type of CRISPR–Cas system that performs dual RNA/DNA targeting activity (14–24). Nevertheless, Csx1 and Csm6 are not found to be associated with any type III effector complexes. Furthermore, they are not required for either RNA cleavage or DNA cleavage by type III effector complexes in vitro (14,16,18,20–22). Although it has been suggested that Csx1/Csm6 is necessary for the transcription-dependent plasmid silencing by Cmr-α in *Sulfolobus islandicus* and Csm in *Staphylococcus epidermidis* respectively (15,25), new evidence shows that they are dispensable for the in vivo DNA targeting by several type III systems (21,26).

Structural and biochemical analyses of Csm6 and Csx1 proteins show that they contain a C-terminal HEPN domain and representative proteins, including *Pyrococcus furiosus* Csx1 and *Thermus thermophilus* Csm6, exhibit metal-independent single-strand (ss)-specific endoribonuclease activity (11,27). It is believed that the ribonuclease activity is performed by the HEPN domain, while the functions of the CARF domain are not understood yet (11,27).

To reveal whether and how CARF domain of Csx1 performs ligand binding and allosteric regulatory function, we characterized the recombinant Csx1 encoded in *S. islandicus* Rey15A (SisCsx1). The results show that the ssRNA cleavage activity of SisCsx1 is activated by 3′-tetra-rA (3′-end four continuous adenosine nucleotides). We further demonstrate that the CARF domain binds to 3′-tetra-rA and regulates the RNase activity of HEPN domain.

MATERIALS AND METHODS

Strains and growth conditions

Genetic hosts *S. islandicus* E233S1 and the *csx1* deletion mutant (*Δcsx1*) were grown in SCVU medium (basic salts and 0.2% sucrose, 0.2% casa amino acids, 1% vitamin solution, 0.2% uracil) at 78°C, while uracil was removed from the medium for transformants. Transformation and construction of *Δcsx1* was performed as described previously (28). The primers used for construction of *Δcsx1* are listed in Supplementary Table S1. *Escherichia coli* DH5α and Rosetta strain were used for plasmid construction and recombinant protein expression in *E. coli*, respectively.

Construction of expression plasmids

To construct pSeSD-based expression plasmid, wild type (WT) *csx1* gene was amplified with the primers SiRe_0884-up-NheI and SiRe_0884-dw-SalI (Supplementary Table S1) and inserted into pSeSD between NheI and SalI. To construct pET30a-based plasmid, the pSeSD-csx1 plasmid was digested by NdeI and SalI, and the gene fragment was purified and inserted into pET30a vector between NdeI and XhoI. Overlapping-PCR was employed to produce *csx1* mutants with the primers listed in Supplementary Table S1, except Csx1M3, which was amplified with SiRe_0884M3-up-NheI and SiRe_0884-dw-SalI (Supplementary Table S1). Then, the mutated gene fragments were inserted into pSeSD and pET30a as the procedure for the wild type gene.

All the primers to be used for DNA cloning were synthesized from Integrated DNA Technology (IDT, USA). Sequences of all plasmid constructs were verified by DNA sequencing at MacroGen Europe (Amsterdam, Netherlands).

Expression and purification of Csx1 and the mutants

The pSeSD-based expression plasmid was transformed into the genetic host E233S1 of *S. islandicus* Rey15A to express WT Csx1, or to Δ*csx1* to express the Csx1 mutants, respectively. The transformants were grown in SCV medium until the optical density of ∼0.2 and then the expression was induced by 0.2% arabinose. However, the expression of Csx1M2 from *S. islandicus* Rey15A was not successful. Therefore, we expressed WT, Csx1M2, M3, M4, M5 and M6 in *E. coli*. For this purpose, the pET30a-based expression plasmids were transformed into *E. coli* Rosetta strain, and the expression was induced by 2.5% lactose at room temperature for overnight.

The purification procedure reported for the purification of native Cmr-α complex was followed with modification (24). Specifically, cell pellet, either *S. islandicus* cells or *E. coli* cells, was re-suspended in Buffer A (20 mM HEPES pH 7.5, 30 mM Imidazole, 500 mM NaCl) and disrupted by French press. The cell extract was loaded onto a 1 ml His-Trap HP (GE) and His-tagged protein was eluted by Buffer B (20 mM HEPES pH 7.5, 500 mM Imidazole, 500 mM NaCl). The Buffer B fractions were concentrated and further purified by size exclusion chromatography in Buffer C (20 mM Tris–HCl pH 7.5, 500 mM NaCl) with a Superdex 200 10/300 GL column (GE). The fractions containing the target protein were pooled, concentrated and used for further analysis.

Size-exclusion chromatography–multi-angle light scattering

The oligomeric state of Csx1 was analyzed by size-exclusion chromatography coupled with multi-angle light scattering (SEC-MALS). Protein samples were prepared at 1 mg/ml concentration and dialyzed into gel filtration running buffer, 20 mM Tris–HCl, 150 mM NaCl, 0.5 mM TCEP, pH 8.0. The samples were loaded on a Superdex 200 Increase 10/300 size exclusion column (GE Healthcare). The column outlet was directly connected to a DAWN HELEOS II MALS detector (Wyatt Technology) followed by an Optilab T-rEX differential refractometer (Wyatt Technology). Data were collected and analysed using ASTRA 6 software (Wyatt Technology). Samples were run in triplicates. The monomeric BSA was used as standard (Sigma-Aldrich).

Labeling of DNA and RNA substrates

RNA and DNA substrates used in cleavage assays were 5′ labeled with ^{32}P using T4 polynucleotide kinase (New England Biolabs). Double strand (ds) DNA was generated by annealing of labeled SS1 ssDNA with unlabeled SS1T ssDNA, while dsRNA was made by annealing of labelled

SS1–40 and SS1–40T (Supplementary Table S2). Then, all substrates were purified by cutting gel from native (dsDNA and dsRNA) or denaturing (ssDNA/RNA) PAGE. The RNA oligos used in the UV crosslink assay were also labeled in a similar way and diluted to 500 nM. Further, the RNA oligos used in the UV crosslink assay have been analyzed by denaturing PAGE to make sure the radioactivity of them was identical. All the DNA and RNA oligos were purchased from IDT, USA.

RNA cleavage assay

To analyze the metal-dependency of SisCsx1-mediated RNA cleavage, labeled SS1–40 was incubated with 3 μM SisCsx1 in the buffer containing 20 mM Mes (pH 6.2) and 5 mM DTT, as well as indicated metal ions or EDTA. For RNA cleavage experiments, the reactions were carried out in the buffer containing 20 mM Mes (pH 6.2), 5 mM $MgCl_2$, 5 mM $MnCl_2$ and 5 mM DTT, as well as indicated substrates, enzyme and unlabeled nucleic acids. The RNA cleavage activity of Cmr-α was performed as previously described (24). To analyze the RNA degradation of a mixture of Cmr-α and Csx1, the two proteins were pre-mixed and then added into the reaction mixture. All the reactions were performed at 70°C and stopped at the indicated time point by supplementing 2 × RNA loading dye (New England Biolabs) and cooling on ice. At last, the samples were heated for 3 min at 95°C and then separated by 18% polyacrylamide denaturing gel and visualized by phosphor imaging. RNA ladders were generated by Decade™ Marker RNA (ambion) following the instructions.

UV crosslink assay

For the UV crosslinking assay, labeled different RNA oligos were incubated with 3 μM SisCsx1 or mutants in the buffer containing 20 mM Mes (pH 6.2), 5 mM $MgCl_2$, 5 mM $MnCl_2$ and 5 mM DTT at 70°C for 10 min, and then exposed to UV irradiation (254 nm) for 30 min in UV stratalinker 1800 (stratagene, USA). The samples were resolved by SDS-loading buffer and heated at 70°C for 5 min. At last, the samples were loaded onto 12% SDS-polyacrylamide gel, and the radioactive signal was visualized by phosphor imaging while the protein band was visualized by Coomassie staining.

Poly(A) polymerase extension assay

To analyze the 3′-end group of the cleavage products generated by SisCsx1, 5′-labeled SS1–40 substrate was incubated with SisCsx1 in the presence of S_3A_7 or not at 70°C for 20 min. Then, half of the reaction mixture was treated with 5 U poly(A) polymerase (PAP, New England Biolabs), 1 mM ATP and 1 × PAP reaction buffer at 37°C for 10 min, while the rest of the reaction mixture was incubated with 1 mM ATP and 1 × PAP reaction buffer as controls. At last, the reactions were stopped by addition of 2 × RNA loading dye (New England Biolabs), heated at 95°C for 3 min and analyzed by 18% polyacrylamide denaturing gel.

RESULTS

The *S. islandicus* Csx1 is a metal-independent single-strand endoribonuclease

The *S. islandicus csx1* gene is located adjacent to the *cas* gene cassette of the III-B Cmr-α system and encodes a Cas accessory protein of 454 amino acids (Supplementary Figure S1). To characterize the encoded protein, the gene was cloned into the *Sulfolobus* expression vector pSeSD, from which a recombinant SisCsx1 protein carrying a 6xHis peptide at the N terminus was expressed. SDS-PAGE analysis of purified SisCsx1 revealed a single protein band of ca. 50 kDa (Figure 1A), while Multi-Angle Laser Light Scattering (MALLS) analysis indicates that SisCsx1 has a size of ∼255 kDa in solution (Figure 1B). The molecular weight of our construct is 53 kDa, suggesting that SisCsx1 could be in a pentameric configuration; however, further analysis is needed to determine the stoichiometry of the oligomer.

RNA cleavage activity of SisCsx1 was tested with the SS1–40 substrate, a single-strand (ss) RNA (RNA protospacer 1 of *lacS* gene) that has been used for characterization of the Cmr-α effector complex (24). To ensure the detection of the RNase activity, a relatively large amount of the purified SisCsx1 protein (3 μM) was mixed with labeled SS1–40 in the presence of Mg^{2+} or Mn^{2+}, or EDTA. The reactions were incubated at 70°C for 60 min, and RNA cleavage products were analyzed by denaturing gel electrophoresis. As shown in Figure 1C, SisCsx1 cleaved the ssRNA substrate under all tested conditions. In contrast, SisCsx1 showed little activity towards a dsRNA molecule generated by annealing SS1–40 with SS1–40T, the complementary RNA (Figure 1D). These results indicated that SisCsx1 is a metal-independent ssRNA-specific ribonuclease.

RNAs carrying a poly(A) tail strongly elevates SisCsx1 RNase activity

Two additional ssRNA substrates (SS1–46 and S10) were tested for SisCsx1 cleavage to further study specificity of RNA cleavage by the enzyme, both of which contain a 6 nt poly(A) tail that is absent from SS1–40 (Supplementary Table S2). Each RNA substrate was incubated with SisCsx1 over time during which samples were taken for RNA cleavage analysis by denaturing gel electrophoresis. Surprisingly, we found that SisCsx1 cleaved about 95% of SS1–46 and S10 in 60 min (Supplementary Figure S2), whereas ∼70% of SS1–40 was cleaved under the same conditions, suggesting that SisCsx1 could be either more active on poly(A) RNA molecules, or poly(A) RNAs could function as an activator to the RNase.

To investigate which scenarios could be true, poly(A)-containing SS1–46 and poly(A)-less SS1–40 were radiolabeled individually, and each labeled substrate was then mixed with 10-fold excess unlabeled SS1–46 or SS1–40 RNA substrate. The mixtures were subsequently used as RNA substrates to examine the cleavage activity of SisCsx1. We found that, while addition of 10-fold excess SS1–40 did not influence the cleavage of labeled SS1–46 or SS1–40, addition of 10-fold excess SS1–46 significantly enhanced the cleavage of both labeled SS1–40 and SS1–46 (Supplementary Figure S3). These results suggested that the poly(A) tail

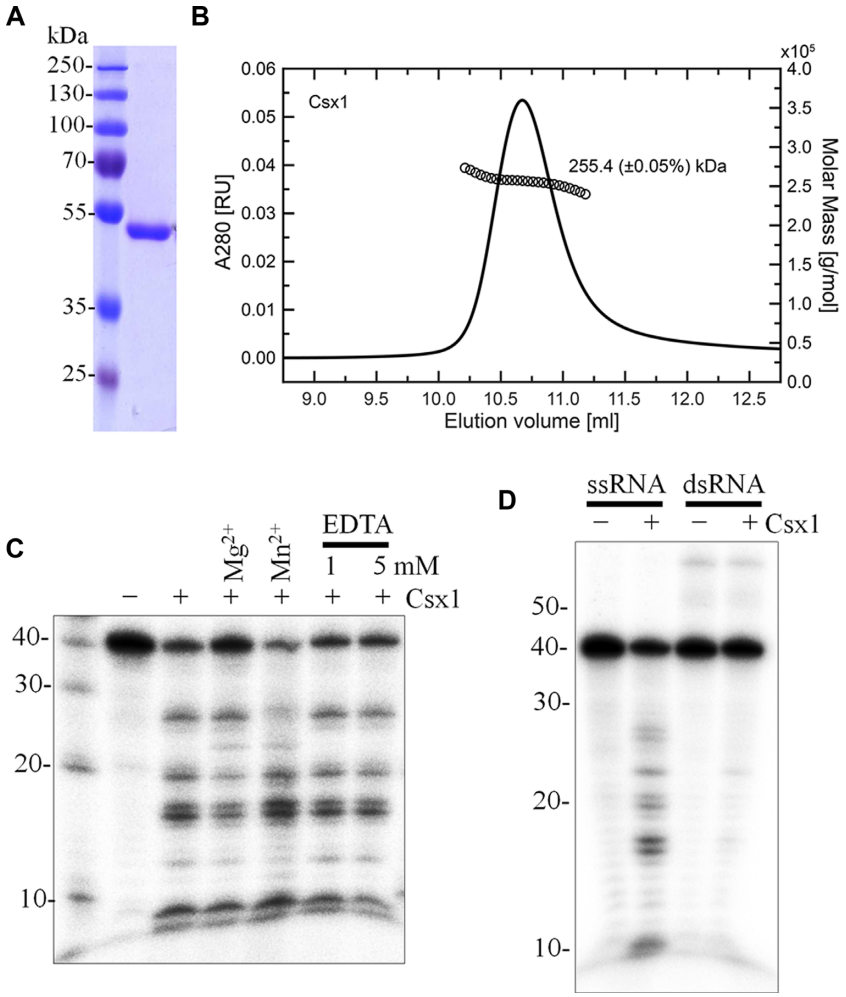

Figure 1. SisCsx1 is a metal-independent single stranded-specific ribonuclease. (**A**) SDS-PAGE analysis of the purified SisCsx1. (**B**) MALS estimation of the size of SisCsx1 in solution. (**C**) The cleavage activity of SisCsx1 is independent of metal ions. Labeled SS1–40 RNA was incubated with 3 μM SisCsx1 for 1 h in the presence of metal ions or EDTA as indicated, followed by separation by denaturing gel electrophoresis. (**D**) ssRNA (SS1–40) and dsRNA (SS1–40+SS1–40T) were incubated with 3 μM SisCsx1 for 40 min and then analyzed by denaturing gel electrophoresis.

present in SS1–46 could function as an activator to the ribonuclease activity of SisCsx1.

The hypothesis was further tested with 5′-S_3A_7–3′ (S–C or G, Supplementary Table S2), a 10-nt RNA oligo containing seven adenosines at the 3′ end. As shown in Figure 2A, in the presence of 200 nM S_3A_7 and a 15-fold lower amount of SisCsx1 (200 nM), all labeled SS1–40 or S10 RNA (25 nM) was cleaved within 20 min of incubation. In comparison, the same amount of the enzyme exhibited little activity on SS1–40 in the absence of S_3A_7. To test if the activation could be poly(A) RNA-specific, several other short RNAs and DNAs were synthesized, including A_7S_3 (seven A at the 5′-end and three C/G at the 3′-end), poly(C) (C_{10}), poly(G) (CG_9), poly(U) (U_{10}), poly(A) DNA (dA_{40}), poly(T) DNA (dT_{40}), poly(C) DNA (dC_{40}), poly(G) DNA (dG_{40}) and ds-DNA (dA_{40}+dT_{40}) and tested for their effects on the Csx1 activity. As shown in Figure 2B and Supplementary Figure S4A, only RNAs containing a poly(A) sequence were capable of activating the SisCsx1 RNase, neither DNAs nor any of the other types of RNA showed any stimulation of the RNase activity. Further, SisCsx1 exhibited higher activity in the presence of S_3A_7 of high concentrations (Supplementary Figure S4B). Together, these results indicated that the RNase activity of SisCsx1 is specifically activated by poly(A) RNAs.

To investigate if the activation of SisCsx1 requires constant presence of the activator, we attempted to separate SisCsx1 from a pre-incubated mixture of SisCsx1 and S_3A_7 by gel filtration chromatography, and analysis of the cleavage activity of protein fractions by incubation with labeled SS1–40 substrate showed that the re-purified SisCsx1 was not active unless the fraction containing S3A7 was added again (Figure 2C and D), indicating that depletion of the poly(A) RNA activator inactivated the enzyme.

Activated SisCsx1 is complementary to the Cmr-α effector complex on RNA cleavage

Next, we analyzed the substrate turnover rate of activated SisCsx1 by supplementing increasing concentrations of unlabeled SS1–40 into the reaction mixture. As shown in Figure 3A and B, the cleavage of SS1–40 exhibited a nearly

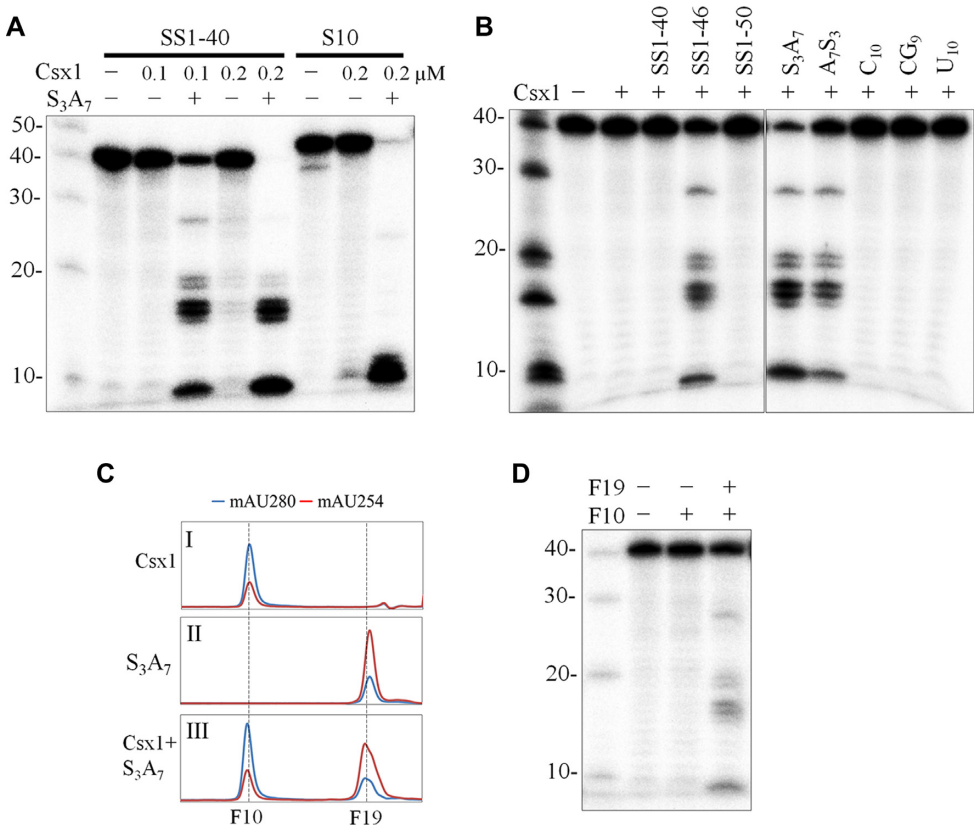

Figure 2. SisCsx1 is activated by poly(A) RNA. (**A**) Labeled SS1–40 and S10 (about 20 nM) were incubated with SisCsx1 at indicated concentration with or without 200 nM S_3A_7 for 20 min. Then, the reactions were stopped and analyzed by denaturing gel electrophoresis. (**B**) Labeled SS1–40 was incubated with 100 nM SisCsx1 in the presence of 200 nM indicated RNA oligos for 20 min, followed by separation by denaturing gel electrophoresis. (**C**) Separation of SisCsx1 and S_3A_7 by gel filtration chromatography. SisCsx1 (panel I), S_3A_7 (panel II) and a mixture of pre-incubated SisCsx1 and S_3A_7 (panel III) were loaded onto a Superdex 200 10/300 GL analytical column, and the UV absorbance at 280 nm and 254 nm was shown. (**D**) Cleavage of SS1–40 by the fractions from the panel III of (C). Labeled SS1–40 was incubated with about 200 nM SisCsx1 from 10-ml fraction or about 200 nM SisCsx1 from 10-ml fraction plus about 200 nM S_3A_7 from 19-ml fraction for 10 min and resolved by denaturing gel electrophoresis.

linear response to increasing substrate concentration until 5 μM, when the molar concentration of substrate is 25 times of SisCsx1 and S_3A_7, indicating a fast turnover rate of SisCsx1 on substrate. This is in contrast to the low turnover rate on target RNA by the type III-B SisCmr-α-SS1 complex (24) where the enzyme was saturated by target RNA of doubled molar concentration (Supplementary Figure S5).

Then, we analyzed the cleavage pattern by mixed SisCmr-α-SS1 and SisCsx1. SS1–40 of different concentrations (25 nM and 5 μM) was cleaved by a mixture of 25 nM SisCmr-α-SS1 and 100 nM SisCsx1 with 500 nM S_3A_7. Separate cleavage by SisCmr-α-SS1 and SisCsx1 with S_3A_7 was also analyzed as references. As shown in Figure 3C, SisCmr-α-SS1 efficiently cleaved the equivalent SS1–40 but hardly degraded 5 μM SS1–40, while SisCsx1 efficiently degraded both 25 nM and 5 μM SS1–40 at almost equal rate. In the presence of both RNases, 25 nM SS1–40 was mostly cleaved by SisCmr-α-SS1 as judged from the distribution of the products, while 5 μM SS1–40 was cleaved by SisCsx1. The data indicate that SisCsx1 did not affect the cleavage of equivalent target RNA by Cmr-α, but efficiently degraded RNA substrate beyond the cleavage capability of Cmr-α, suggesting that SisCsx1 plays a complementary role to Cmr-α.

The HEPN domain is responsible for basal and activated RNA cleavage activity

We showed that SisCsx1 exhibits ribonuclease activity at two distinct levels, i.e. the basal level and the activated level in the presence of an RNA activator. Previous studies revealed that a conserved motif, R-X_{4-6}-H, located in the C-terminal HEPN domain is important for the ribonuclease activity of Csx1 and Csm6 (11,27). Here, we investigated whether the SisCsx1 HEPN domain could also be responsible for the ribonuclease activity. Two alanine mutations were introduced to the well-conserved arginine and histidine residues in the R-X_{4-6}-H motif of the HEPN domain, giving Csx1M1 (Supplementary Figures S6 and S7). The resulting mutant gene was expressed in *S. islandicus* as recombinant protein and assayed for RNA cleavage. The results showed that Csx1M1 became inactive in RNA hydrolysis, even at a relatively high concentration (1 μM) or in the presence of the activator S_3A_7 (Figure 4A), indicating that both the basal and the activated ribonuclease activity of SisCsx1 resides in the HEPN domain.

Next, substrate specificity of the enzyme was investigated in the presence of the S_3A_7 activator with different forms of nucleic acids, including ssRNA, dsRNA, ssDNA and dsDNA. As in the absence of any activator, SisCsx1 only de-

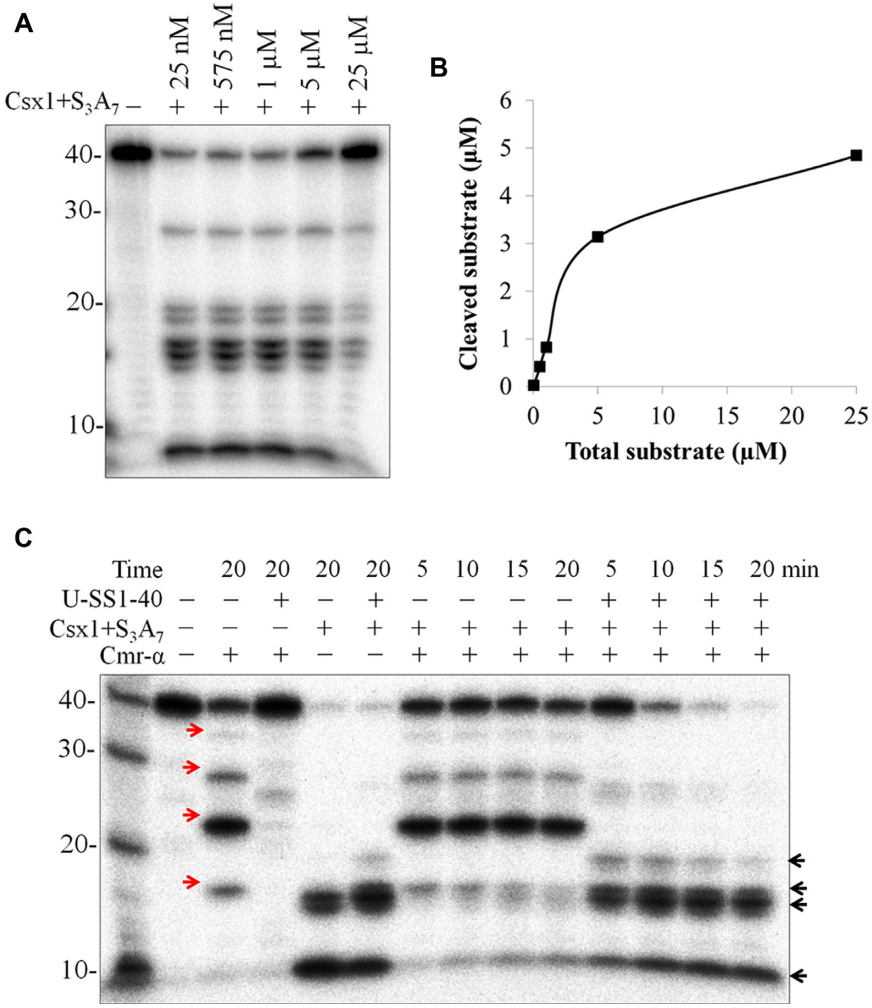

Figure 3. Activated SisCsx1 exhibits fast substrate turnover rate. (**A**) Labeled and unlabeled SS1–40 (total concentration as indicated) was incubated with 200 nM SisCsx1 for 10 min in the presence of 200 nM S_3A_7, and then separated by denaturing gel electrophoresis. (**B**) Quantification of cleaved substrate from (A). (**C**) Competitive cleavage of SS1–40 by SisCmr-α-SS1 and SisCsx1. Labeled SS1–40 (25 nM) with or without unlabeled SS1–40 (U-SS1–40, 5 μM) as indicated was incubated with SisCmr-α-SS1 and SisCsx1 in the presence of 500 nM S_3A_7 for indicated times, followed by analysis by denaturing gel electrophoresis. Cleavage by SisCmr-α-SS1 and SisCsx1 separately was also analyzed as references. The red and black arrows indicate the products by SisCmr-α-SS1 and SisCsx1, respectively.

graded ssRNA (Figure 4B), indicating that poly(A) RNA activator does not have any influence on substrate specificity of the enzyme.

Previous studies showed that Csx1/Csm6 yield products carrying a 2′,3′-cyclic phosphate or 3′-phosphate and 5′-OH group (11,27). To analyze whether SisCsx1 could possess the same cleavage property, the 3′-end group of the cleavage products generated by SisCsx1 was analyzed using poly(A) polymerase (PAP) extension assay as reported previously (27) since PAP is capable to add poly(A) tail to any RNA that carries the 3′-OH group. 5′-labeled SS1–40 was cleaved by SisCsx1, and the resulting cleavage products were treated with PAP and ATP for 10 min. Analysis of RNAs in the reactions by denaturing gel electrophoresis showed that, while uncleaved substrate was extended by PAP, none of the cleavage products were extended (Figure 4C), indicating that all the products lack the 3′-OH group. Therefore, cleavage products generated by SisCsx1 should carry the same end groups as for the products generated by other known HEPN domain nucleases. Further, SisCsx1 produced the same cleavage products in the presence or absence of S_3A_7 RNA activator, indicating that the RNA did not influence the cleavage pattern of the enzyme.

Activation of SisCsx1 RNase requires an RNA carrying 4 nt poly(A) tail

To determine the minimal requirement of an RNA activator for SisCsx1, four additional 10 nt RNAs were synthesized, i.e. S_8A_2, S_7A_3, S_6A_4 and S_5A_5. Investigation of their capability to facilitate SisCsx1 RNase activity showed that while the enzyme failed to cleave the SS1–40 substrate in the presence of S_8A_2 and S_7A_3 (Figure 5A and B), S_6A_4, S_5A_5 and S_3A_7 strongly activated SS1–40 cleavage by SisCsx1, and furthermore, the activation was equally efficient by the three RNA activators carrying four, five or seven adenosines at the 3′-end (Figure 5A and B). The results indicated that the minimal size of poly(A) in an RNA activator is 4 nt and

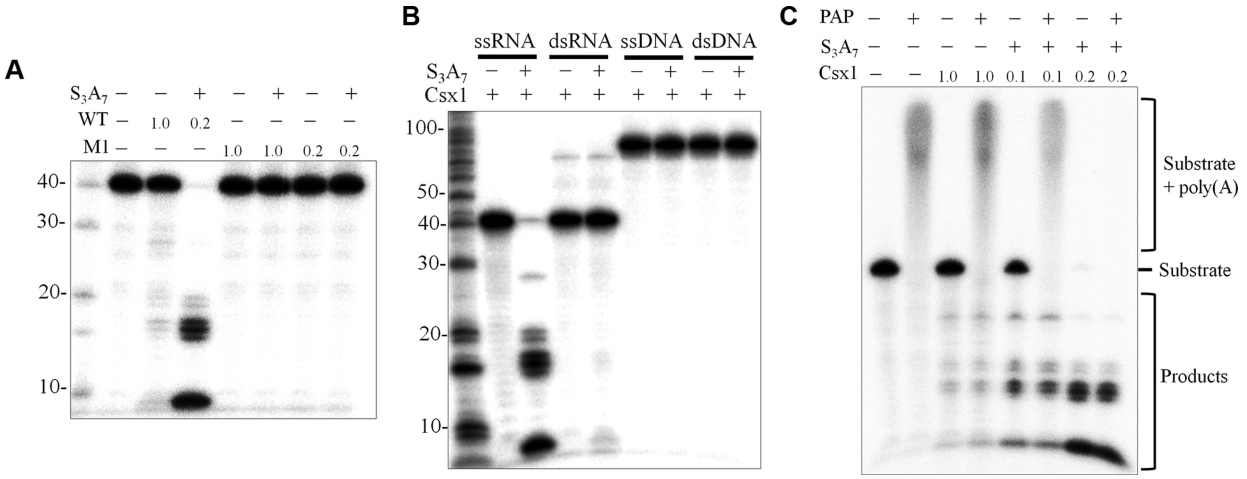

Figure 4. (**A**) HEPN domain mutation abolished the RNA cleavage activity of SisCsx1. Labeled SS1–40 was incubated with Csx1-WT and Csx1-M1 (R399A, H404A) at indicated concentrations with or without S_3A_7 for 20 min, and then separated by denaturing gel electrophoresis. (**B**) SisCsx1 is a single-strand specific ribonuclease in the presence of S_3A_7. Different substrates (ssRNA: SS1–40, dsRNA: SS1–40+SS1–40T, ssDNA: SS1 DNA, dsDNA: SS1+SS1T DNA) were tested for the nuclease activity of Csx1 with or without 200 nM S_3A_7. The sequences of the substrates were listed in Supplementary Table S2. Size standard (M) is measured in nucleotides. (C) Products of SisCsx1 cleavage lack 3′-end OH group. Labeled SS1–40 was incubated with SisCsx1 at indicated concentrations with or without S_3A_7 for 20 min, and then treated with PAP for 10 min, followed by separation by denaturing gel electrophoresis.

the presence of additional adenosine nucleotides (>4 nt) in RNA activators does not further enhance the activation.

To address whether additional 3′-end non-adenosine nucleotides would affect SisCsx1 activation, five additional RNA oligos were synthesized, i.e. CA_4 carrying an 3′-OH group, CA_4-p containing a 3′ phosphate group, and CA_4S_1, CA_4S_3 and CA_4S_6 that carry one, three or six additional C or G nucleotides at the 3′-end, respectively. Analysis of SisCsx1 activity in the presence of each of these RNAs showed that addition of one or more nucleotides at 3′-end significantly impaired the activation, indicating that SisCsx1 activation requires a 3′-poly(A) tail (Figure 5C).

Then, modifications of poly(A) in CA_4 were designed to yield an additional insight into the activation mechanisms, including 4 variants lacking 2′-hydroxyl group at different positions (CA_3-dA, CA_2-dA-A, CA-dA-A_2, C-dA-A_3), one phosphorothioate backbone modification in which a non-bridging oxygen of the sugar-phosphate linkage is replaced with a sulfur atom between each two of the four adenosines (C*A_4). Each of these RNAs was tested for SisCsx1 RNase activation, and we found that none of them were capable of activating the SisCsx1 RNase (Figure 5C). Together, the results indicated that the integrity of 3′-tetra-rA is essential for the activation.

RNA activators bind to SisCsx1 as a ligand

The activation of SisCsx1 by 3′-poly(A) RNA suggested that SisCsx1 could bind to the poly(A) tail of a RNA molecule as ligand to allosterically regulate the RNase activity. To test the hypothesis, the electrophoretic mobility shift assay (EMSA) was employed to detect the formation of RNA-protein complexes. As shown in Supplementary Figure S8, the labeled S_3A_7 did not show any retardation in migration in the presence of excess SisCsx1 (4.5 μM), indicating that the interaction between SisCsx1 and the RNA ligand could be weak. Then, UV cross-link assay was employed to investigate the interaction of SisCsx1 and 3′-poly(A) RNA. SisCsx1 was incubated with increasing concentrations of unlabeled S_3A_7 and exposed to UV irradiation, and the samples were then analyzed by SDS-PAGE. The results showed that in the absence of any RNA ligand, UV irradiation yielded additional protein bands that appeared either larger or smaller than the original SisCsx1 protein, and in the presence of an excess amount of RNA ligand S_3A_7 (50 μM), UV radiation produced a new band corresponding to the size of SisCsx1 dimer, suggesting that two SisCsx1 molecules were crosslinked together in the presence of the S_3A_7 ligand (Figure 6A).

We further compared the interaction of SisCsx1 with S_3A_7 and a few non-activator RNAs by UV crosslink. Labeled RNA oligos were incubated with SisCsx1, followed by UV irradiation. Then, the samples were analyzed by SDS-PAGE and visualized by phosphor imaging and Coomassie blue staining. The results showed that S_3A_7 was associated with SisCsx1 in the SDS-polyacrylamide gel, while a much lower level of C_{10}, CG_9, U_{10}, S_7A_3 and A_7S_3 were observed to associate with SisCsx1, suggesting that SisCsx1 specifically binds to 3′-end poly(A) RNA (Figure 6B). These results were in good agreement with those obtained from their RNase assay.

Next, we analyzed the affinity of CA_4 and its variants to SisCsx1, and this revealed that addition of one or more nucleotides at 3′-end significantly reduced the affinity to SisCsx1, in agreement with their effects on SisCsx1 activity (Figure 6C). However, removal of 2′-hydroxyl group of each adenosine or phosphorothioate modification of the RNA ligand greatly weakened or abolished the activation of SisCsx1 although these RNAs showed an elevated affinity to the protein (Figure 6C). Taken together, the data indicated that binding to RNA ligand is necessary but not sufficient for SisCsx1 activation.

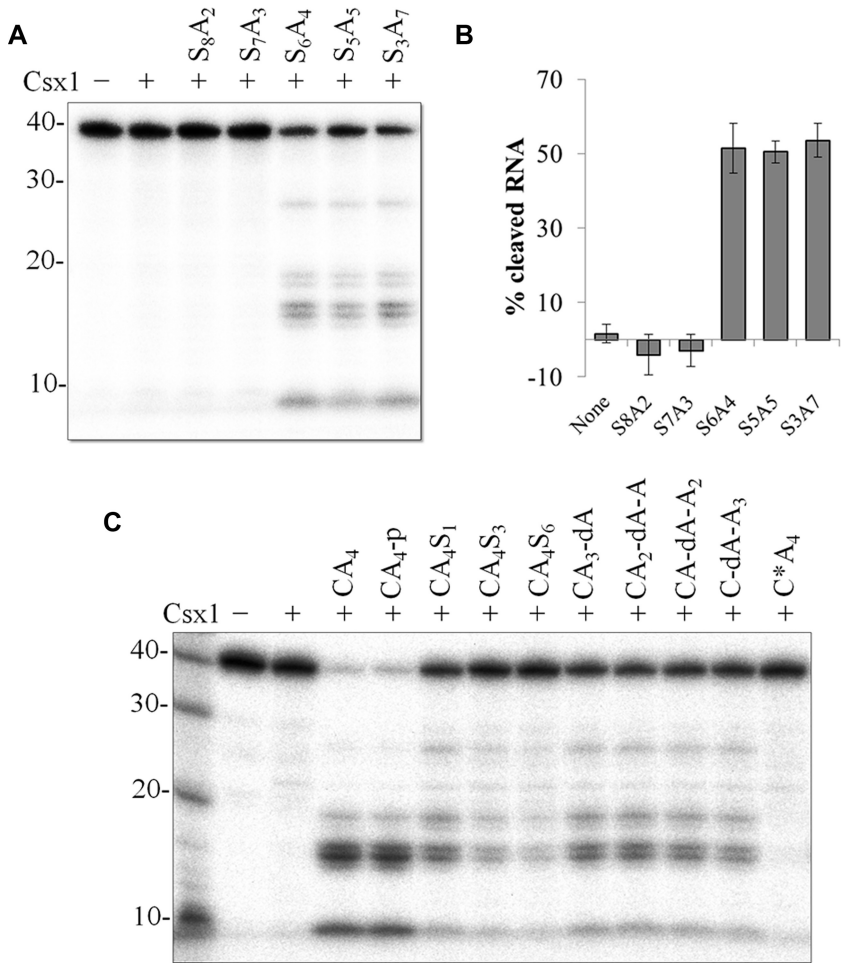

Figure 5. Determination of the activator for SisCsx1. (**A**) Activation of SisCsx1 requires four adenosines. Labeled SS1–40 was incubated with 100 nM SisCsx1 with 2 μM S_8A_2, S_7A_3, or 200 nM S_6A_4, S_5A_5 and S_3A_7 or without any short RNA oligo, followed by denaturing gel electrophoresis. (**B**) Quantification of the percentage of cleaved substrate from (A). 'None' means no 10-nt RNA oligo. Error bar represents S.D. of three independent experiments. (**C**) Labeled SS1–40 was incubated with 200 nM SisCsx1 with 200 nM CA_4 and its variants (Supplementary Table S2) for 20 min and analyzed by denaturing gel electrophoresis.

The CARF domain is responsible for ligand binding

The CARF domain of Csx1 contains a predicted ligand-binding site (12). It was reported that Csx3, a single domain protein of the CARF superfamily, co-crystallizes with tetranucleotides (9,29). To investigate if SisCsx1 CARF domain could be responsible for binding of poly(A) RNA and for regulation of the RNase activity in the HEPN domain, we expressed five Csx1 mutants carrying mutations in the conserved amino acids of the CARF domain (Supplementary Figures S6 and S7), i.e. Csx1-M2 (G95L-A97L-A99L), M3 (D50L-S51L), M4 (G9L), M5 (G156L) and M6 (H155L). These mutant proteins were expressed and purified from *E. coli* (Supplementary Figure S7) since attempts to produce them from *S. islandicus* failed. These Csx1 proteins were individually incubated with label SS1–40 substrate in the absence of S_3A_7 to analyze their basal ribonuclease activity, and this revealed that all CARF mutants possessed an RNA cleavage activity comparable to the WT enzyme at the concentration of 1 μM (Figure 7A). However, when reduced to 200 nM, none of the mutant enzymes exhibited a detectable cleavage activity in the presence of S3A7, suggesting that they all lost the capability to be activated by poly(A) RNA (Figure 7B). Further, UV crosslink assay revealed that, while M4 and M5 exhibited a lower affinity to S_3A_7 compared to WT, the binding of S_3A_7 to M2, M3 and M6 went to an undetectable level (Figure 7C). In contrast, HEPN mutation did not affect the affinity of the mutant enzyme to S_3A_7 (Supplementary Figure S9). Taken together, the data indicated that the conserved amino acids in the CARF domain are responsible for ligand binding and/or allosteric regulation to activate the RNase activity of the HEPN domain.

DISCUSSION

In this study, we have characterized the *S. islandicus* Csx1, a type III-B-associated Cas accessory protein that contains a CARF and a HEPN domain. Functional analyses of the two domains have revealed that the CARF domain can bind to an RNA ligand carrying a tetraadenylate tail and that the ligand binding activates the RNA cleavage by the HEPN domain.

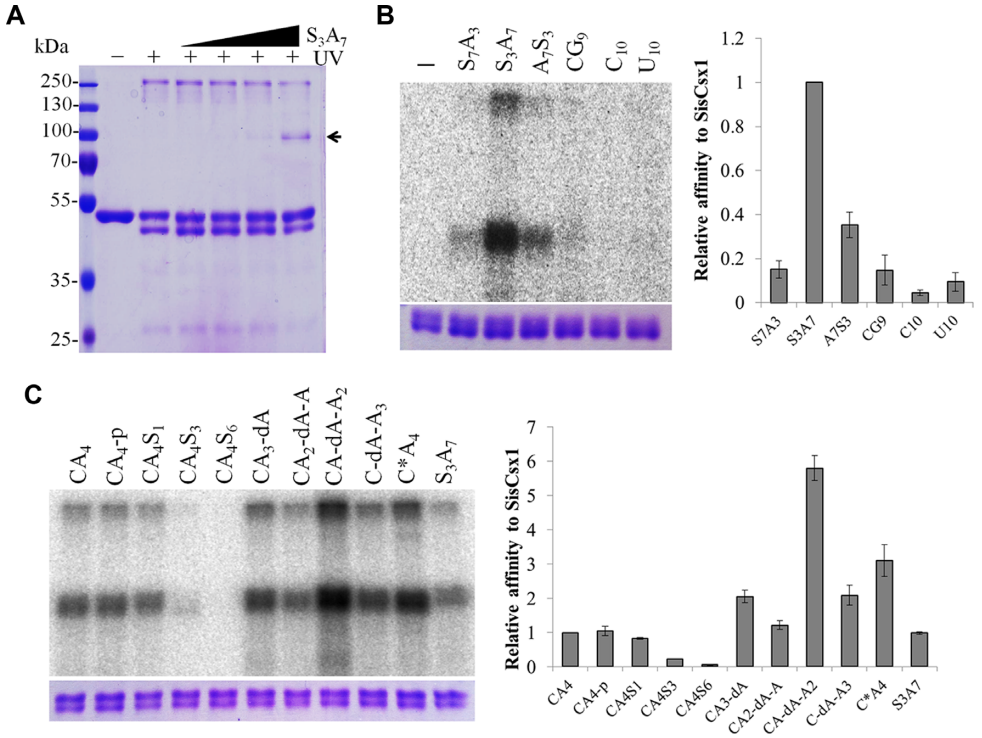

Figure 6. UV cross-link analysis of the interaction between SisCsx1 and different RNA oligos. (**A**) SisCsx1 (3 μM) was incubated with increasing concentrations of S_3A_7 (0, 0.1, 1, 10, 50 μM) at 70°C for 10 min and exposed to UV irradiation for 30 min. Then, the samples were resolved by SDS-loading buffer, analyzed by SDS-PAGE and visualized by Coomassie staining. (**B** and **C**) Labeled indicated RNA oligos (Supplementary Table S2) were incubated with 3 μM SisCsx1 at 70°C for 10 min and exposed to UV irradiation for 30 min. Then the samples were loaded onto a SDS-polyacrylamide gel and analyzed by autoradiography (upper panel) and Coomassie staining (lower panel). The right panels show the relative amount of the indicated RNA oligos bound by SisCsx1. Only the signal from the main band was calculated and the amount of Csx1-associated S_3A_7 and CA_4 was set as '1' in (B) and (C), respectively.

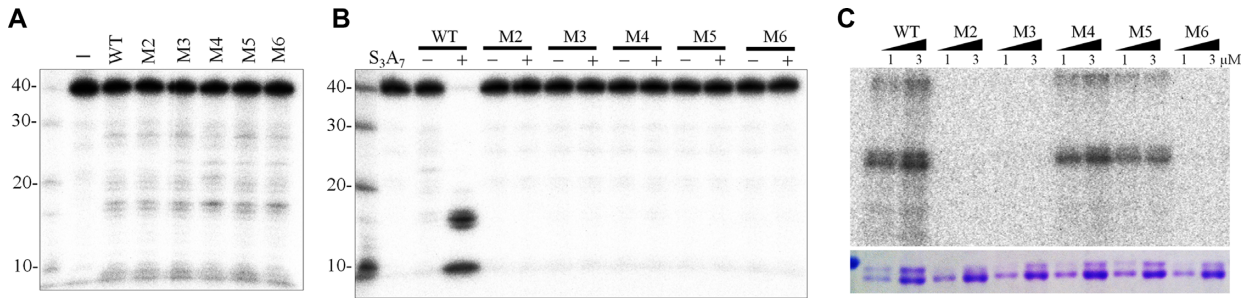

Figure 7. CARF domain of SisCsx1 is responsible for the activation of ribonuclease activity by binding to poly(A) RNA ligand. (**A**) CARF domain mutations (M2: G95L-A97L-A99L, M3: D50L-S51L, M4: G9L, M5: G156L, M6: H155L) did not affect the RNA cleavage activity in the absence of poly(A) RNA. Labeled SS1–40 was incubated with 1 μM of Csx1-WT and Csx1-M2, M3, M4, M5, M6 for 20 min and then separated by denaturing gel electrophoresis. (**B**) CARF domain mutations abolished the activation of the RNA cleavage activity by S_3A_7. Labeled SS1–40 was incubated with 200 nM of Csx1-WT and Csx1-M2, M3, M4, M5, M6 for 20 min with or without 200 nM S_3A_7 and then separated by denaturing gel electrophoresis. (**C**) UV cross-link assay analysis of the affinity of CARF domain mutations to S_3A_7 with WT as a positive control. UV cross-link assay was performed as described in Figure 6.

The tetraadenylate RNA ligand was discovered accidentally. When two categories of RNA, which were used to demonstrate the RNA-activated DNA cleavage by Cmr-α in a previous work (24), were employed as substrate to investigate the SisCsx1 RNase activity, i.e. the cognate target RNAs carrying a 6 nt 3′-poly(A) tail in the corresponding position of the repeat tag (SS1–46 and S10) and the repeat tag-less target RNA (SS1–40), we found that SisCsx1 exhibits a higher activity to RNAs containing a poly(A) tail compared with non-poly(A) RNAs, and this suggests that poly(A) RNAs can strongly activate the basal RNase activity of SisCsx1. This hypothesis was then tested with a series of small RNAs, and this has revealed that an activator RNA should carry at least 4-nt adenosines at the 3′-tail. We further show that SisCsx1 directly binds to the RNA ligand. The ligand-enzyme interaction is dependent on the CARF domain of SisCsx1, and the ligand-binding is required to activate the RNA cleavage activity by the HEPN domain.

Moreover, poly(A) segment at 5′-end or in the middle of small RNAs exhibits much lower affinity to SisCsx1 and significantly reduced capability to stimulate the enzyme, suggesting that the RNA ligand could be recognized by the enzyme from 3′-end. In addition, the 2′-OH groups of poly(A) adenosines are not important for ligand binding but essential for enzyme activation, revealing additional insight to the mechanisms of the allosteric regulation of SisCsx1 activity.

We have also revealed that the interaction between the poly(A) RNA ligand and SisCsx1 is rather dynamic and dissociation of RNA ligands from the enzyme can result in an almost inactive enzyme. The findings imply that SisCsx1 could be activated by RNA polyadenylation and inactivated by degradation of 3′-poly(A) RNAs. Interestingly, this is consistent with the RNA decay pathway present in most prokaryotes, which functions in two consecutive steps: addition of 3′-poly(A) tail onto RNA (RNA polyadenylation) and degradation polyadenylated RNA (30–32). To this end, it is tempting to assume that poly(A) RNAs synthesized by exosomes in *Sulfolobus* readily activates Csx1. Since tetraadenylate-Csx1 interaction is dynamic, this renders it possible for the archaeon to readily activate the enzyme when polyadenylated RNAs are abundant and to readily inactivate the enzyme when poly(A) RNAs are degraded. Strikingly, recent study on the regulation of RNA polyadenylation in *S. solfataricus* has shown that DnaG and SmAP proteins enhance RNA polyadenylation activity (33,34), and these data provide not only the first examples of regulation of RNA polyadenylation in response to cellular stresses, but also a mechanism of allosteric regulation of Csx1 by poly(A) RNAs in vivo.

Furthermore, transcripts in prokaryotes end up with U-rich tail (35,36), which could avoid activation of Csx1 at normal growing conditions. In addition, the widespread CARF domain toxins, i.e. CARF domain proteins carrying a C-terminal nuclease domain (6), are absent in halobacteria (Supplementary Table S3), an archaeal class that lack RNA polyadenylation (32), providing an indirect evidence supporting that regulation of Csx1 and other CARF domain toxins is related to RNA polyadenylation.

Most recently, it has been reported that type III-A effector Csm complex synthesizes a cyclic oligonucleotide upon binding to target RNA and that the cyclic oligonucleotide activates the ribonuclease activity of type III-A associated Csm6 protein (37,38). The Csm6 activation is strictly dependent on an active type III-A effector complex, the presence of a spacer matching viral genome and the transcription of the protospacer (37). Therefore, the response is highly specific. However, in another report, RNA cleavage activity by Csm6 was found to be essential for the type III-A-mediated antiviral immunity when the protospacer is from a late-expressed gene or when the protospacer is mutated (26). Since the Csm effector complex cannot synthesize the cyclic oligonucleotide required for Csm6 activation either in a timely fashion or effectively under those conditions (37), this suggests that an alternative mechanism is required for Csm6 activation to yield the observed results. In this respect, another RNA ligand such as poly(A) could have played the role instead of the cyclic oligonucleotide. Indeed, it has been shown that the RNase activity of Csm6 can also been strongly activated by poly(A) RNAs (38). Together, these data suggest that the tetraadenylate activation of CARF-domain RNases is evolutionarily conserved in Bacteria and Archaea although it remains to be demonstrated whether the cyclic oligoadenylate synthesis is conserved in other type III CRISPR–Cas systems.

On the other hand, genes coding for CARF domain nucleases are dispersed in bacterial and archaeal genomes, a number of which are not associated with type III CRISPR–Cas systems (6,10). Our finding that poly(A) RNAs can function as an activator to the *S. islandicus* SisCsx1 can be generally applied to all CARF domain nucleases regardless whether they are associated with any CRISPR–Cas systems. Thus, RNA polyadenylation-dependent activation of CARF domain nucleases presents an alternative mechanism of enzyme activation.

Indeed, SisCsx1 cleaves unspecific ssRNA substrates with a high turnover rate, which is in contrast to the low turnover RNA cleavage by Cmr-α. Therefore, SisCsx1 can have more important roles in destruction of viral transcripts to limit the infectious cycle, relative to the III-B Cmr-α system. Furthermore, the rapid destruction of ssRNAs by activated SisCsx1 exhibits a good potential to degrade large amounts of host mRNAs, leading to growth inhibition, cell dormancy or even cell death of the host as well as to prevention of virus replication and spreading (39). In eukaryotes, it has been shown that a ubiquitous RNase, RNase L is activated by 2′-5′ oligoadenylate upon virus infection and the enzyme is responsible for degradation both viral and host RNA and induce autophagy and apoptosis (40,41). Although it remains to be demonstrated, several prokaryotic RNases could play a similar role, and these include Csm6 proteins from several bacterial species (37,38) and their distant homolog SisCsx1 from a hyperthermophilic archaeon reported here, and probably all identified Csx1/Csm6 homologs (6). Therefore, allosteric regulation of RNase activity may represent a general strategy for antiviral defense in all three domains of life.

SUPPLEMENTARY DATA

Supplementary Data are available at NAR Online.

ACKNOWLEDGEMENTS

We thank members of both laboratories for stimulating discussions.

FUNDING

Danish Council for Independent Research [DFF-0602-02196, DFF-1323-00330]; The Augustinus Foundation [15-3934]; Brødrene Hartmanns Foundation [A29992]; Natural Science Foundation of China [31128011]; Scientific and Technological Self-Innovation Foundation of Huazhong Agricultural University [2014RC011 to Q.S.]. The Novo Nordisk Foundation Center for Protein Research is supported financially by the Novo Nordisk Foundation [NNF14CC0001]; Danish Cancer Society (to G.M.). Funding for open access charge: University of Copenhagen.

Conflict of interest statement. None declared.

REFERENCES

1. Deveau,H., Garneau,J.E. and Moineau,S. (2010) CRISPR/Cas system and its role in phage-bacteria interactions. *Annu. Rev. Microbiol.*, **64**, 475–493.
2. Marraffini,L.A. and Sontheimer,E.J. (2010) CRISPR interference: RNA-directed adaptive immunity in bacteria and archaea. *Nat. Rev. Genet.*, **11**, 181–190.
3. Heler,R., Marraffini,L.A. and Bikard,D. (2014) Adapting to new threats: the generation of memory by CRISPR–Cas immune systems. *Mol. Microbiol.*, **93**, 1–9.
4. Makarova,K.S., Haft,D.H., Barrangou,R., Brouns,S.J., Charpentier,E., Horvath,P., Moineau,S., Mojica,F.J., Wolf,Y.I., Yakunin,A.F. *et al.* (2011) Evolution and classification of the CRISPR–Cas systems. *Nat. Rev. Microbiol.*, **9**, 467–477.
5. Mohanraju,P., Makarova,K.S., Zetsche,B., Zhang,F., Koonin,E.V. and van der Oost,J. (2016) Diverse evolutionary roots and mechanistic variations of the CRISPR–Cas systems. *Science*, **353**, aad5147.
6. Makarova,K.S., Anantharaman,V., Grishin,N.V., Koonin,E.V. and Aravind,L. (2014) CARF and WYL domains: ligand-binding regulators of prokaryotic defense systems. *Front. Genet.*, **5**, 102.
7. Haft,D.H., Selengut,J., Mongodin,E.F. and Nelson,K.E. (2005) A guild of 45 CRISPR-associated (Cas) protein families and multiple CRISPR/Cas subtypes exist in prokaryotic genomes. *PLoS Comput. Biol.*, **1**, e60.
8. Makarova,K.S., Grishin,N.V., Shabalina,S.A., Wolf,Y.I. and Koonin,E.V. (2006) A putative RNA-interference-based immune system in prokaryotes: computational analysis of the predicted enzymatic machinery, functional analogies with eukaryotic RNAi, and hypothetical mechanisms of action. *Biol. Direct.*, **1**, 7.
9. Topuzlu,E. and Lawrence,C.M. (2016) Recognition of a pseudo-symmetric RNA tetranucleotide by Csx3, a new member of the CRISPR associated Rossmann fold superfamily. *RNA Biol.*, **13**, 254–257.
10. Lintner,N.G., Frankel,K.A., Tsutakawa,S.E., Alsbury,D.L., Copie,V., Young,M.J., Tainer,J.A. and Lawrence,C.M. (2011) The structure of the CRISPR-associated protein Csa3 provides insight into the regulation of the CRISPR/Cas system. *J. Mol. Biol.*, **405**, 939–955.
11. Niewoehner,O. and Jinek,M. (2016) Structural basis for the endoribonuclease activity of the type III-A CRISPR-associated protein Csm6. *RNA*, **22**, 318–329.
12. Kim,Y.K., Kim,Y.G. and Oh,B.H. (2013) Crystal structure and nucleic acid-binding activity of the CRISPR-associated protein Csx1 of Pyrococcus furiosus. *Proteins*, **81**, 261–270.
13. Vestergaard,G., Garrett,R.A. and Shah,S.A. (2014) CRISPR adaptive immune systems of Archaea. *RNA Biol.*, **11**, 156–167.
14. Hale,C.R., Zhao,P., Olson,S., Duff,M.O., Graveley,B.R., Wells,L., Terns,R.M. and Terns,M.P. (2009) RNA-guided RNA cleavage by a CRISPR RNA-Cas protein complex. *Cell*, **139**, 945–956.
15. Deng,L., Garrett,R.A., Shah,S.A., Peng,X. and She,Q. (2013) A novel interference mechanism by a type IIIB CRISPR-Cmr module in Sulfolobus. *Mol. Microbiol.*, **87**, 1088–1099.
16. Staals,R.H., Agari,Y., Maki-Yonekura,S., Zhu,Y., Taylor,D.W., van Duijn,E., Barendregt,A., Vlot,M., Koehorst,J.J., Sakamoto,K. *et al.* (2013) Structure and activity of the RNA-targeting Type III-B CRISPR–Cas complex of Thermus thermophilus. *Mol. Cell*, **52**, 135–145.
17. Goldberg,G.W., Jiang,W., Bikard,D. and Marraffini,L.A. (2014) Conditional tolerance of temperate phages via transcription-dependent CRISPR–Cas targeting. *Nature*, **514**, 633–637.
18. Tamulaitis,G., Kazlauskiene,M., Manakova,E., Venclovas,C., Nwokeoji,A.O., Dickman,M.J., Horvath,P. and Siksnys,V. (2014) Programmable RNA shredding by the type III-A CRISPR–Cas system of Streptococcus thermophilus. *Mol. Cell*, **56**, 506–517.
19. Peng,W., Feng,M., Feng,X., Liang,Y.X. and She,Q. (2015) An archaeal CRISPR type III-B system exhibiting distinctive RNA targeting features and mediating dual RNA and DNA interference. *Nucleic Acids Res.*, **43**, 406–417.
20. Samai,P., Pyenson,N., Jiang,W., Goldberg,G.W., Hatoum-Aslan,A. and Marraffini,L.A. (2015) Co-transcriptional DNA and RNA Cleavage during Type III CRISPR–Cas Immunity. *Cell*, **161**, 1164–1174.
21. Elmore,J.R., Sheppard,N.F., Ramia,N., Deighan,T., Li,H., Terns,R.M. and Terns,M.P. (2016) Bipartite recognition of target RNAs activates DNA cleavage by the Type III-B CRISPR–Cas system. *Genes Dev.*, **30**, 447–459.
22. Estrella,M.A., Kuo,F.T. and Bailey,S. (2016) RNA-activated DNA cleavage by the Type III-B CRISPR–Cas effector complex. *Genes Dev.*, **30**, 460–470.
23. Kazlauskiene,M., Tamulaitis,G., Kostiuk,G., Venclovas,C. and Siksnys,V. (2016) Spatiotemporal control of type III-A CRISPR–Cas immunity: coupling DNA degradation with the target RNA Recognition. *Mol Cell*, **62**, 295–306.
24. Han,W., Li,Y., Deng,L., Feng,M., Peng,W., Hallstrom,S., Zhang,J., Peng,N., Liang,Y.X., White,M.F. *et al.* (2016) A type III-B CRISPR–Cas effector complex mediating massive target DNA destruction. *Nucleic Acids Res.*, **45**, 1983–1993.
25. Hatoum-Aslan,A., Maniv,I., Samai,P. and Marraffini,L.A. (2014) Genetic characterization of antiplasmid immunity through a type III-A CRISPR–Cas system. *J. Bacteriol.*, **196**, 310–317.
26. Jiang,W., Samai,P. and Marraffini,L.A. (2016) Degradation of phage transcripts by CRISPR-associated RNases enables type III CRISPR–Cas immunity. *Cell*, **164**, 710–721.
27. Sheppard,N.F., Glover,C.V. 3rd, Terns,R.M. and Terns,M.P. (2016) The CRISPR-associated Csx1 protein of Pyrococcus furiosus is an adenosine-specific endoribonuclease. *RNA*, **22**, 216–224.
28. She,Q., Zhang,C., Deng,L., Peng,N., Chen,Z. and Liang,Y.X. (2009) Genetic analyses in the hyperthermophilic archaeon Sulfolobus islandicus. *Biochem. Soc. Trans.*, **37**, 92–96.
29. Yan,X., Guo,W. and Yuan,Y.A. (2015) Crystal structures of CRISPR-associated Csx3 reveal a manganese-dependent deadenylation exoribonuclease. *RNA Biol.*, **12**, 749–760.
30. Schuster,G. and Stern,D. (2009) RNA polyadenylation and decay in mitochondria and chloroplasts. *Prog. Mol. Biol. Transl. Sci.*, **85**, 393–422.
31. Dreyfus,M. and Regnier,P. (2002) The poly(A) tail of mRNAs: bodyguard in eukaryotes, scavenger in bacteria. *Cell*, **111**, 611–613.
32. Portnoy,V., Evguenieva-Hackenberg,E., Klein,F., Walter,P., Lorentzen,E., Klug,G. and Schuster,G. (2005) RNA polyadenylation in Archaea: not observed in Haloferax while the exosome polynucleotidylates RNA in Sulfolobus. *EMBO Rep.*, **6**, 1188–1193.
33. Hou,L., Klug,G. and Evguenieva-Hackenberg,E. (2014) Archaeal DnaG contains a conserved N-terminal RNA-binding domain and enables tailing of rRNA by the exosome. *Nucleic Acids Res.*, **42**, 12691–12706.
34. Martens,B., Hou,L., Amman,F., Wolfinger,M.T., Evguenieva-Hackenberg,E. and Blasi,U. (2017) The SmAP1/2 proteins of the crenarchaeon Sulfolobus solfataricus interact with the exosome and stimulate A-rich tailing of transcripts. *Nucleic Acids Res.*, doi:10.1093/nar/gkx437.
35. Dar,D., Prasse,D., Schmitz,R.A. and Sorek,R. (2016) Widespread formation of alternative 3′ UTR isoforms via transcription termination in archaea. *Nat. Microbiol.*, **1**, 16143.
36. Ray-Soni,A., Bellecourt,M.J. and Landick,R. (2016) Mechanisms of bacterial transcription termination: all good things must end. *Annu. Rev. Biochem.*, **85**, 319–347.
37. Kazlauskiene,M., Kostiuk,G., Venclovas,C., Tamulaitis,G. and Siksnys,V. (2017) A cyclic oligonucleotide signaling pathway in type III CRISPR–Cas systems. *Science*, **357**, 605–609.
38. Niewoehner,O., Garcia-Doval,C., Rostol,J.T., Berk,C., Schwede,F., Bigler,L., Hall,J., Marraffini,L.A. and Jinek,M. (2017) Type III CRISPR–Cas systems produce cyclic oligoadenylate second messengers. *Nature*, doi:10.1038/nature23467.
39. Koonin,E.V. and Zhang,F. (2017) Coupling immunity and programmed cell suicide in prokaryotes: life-or-death choices. *Bioessays*, **39**, 1–9.
40. Tanaka,N., Nakanishi,M., Kusakabe,Y., Goto,Y., Kitade,Y. and Nakamura,K.T. (2004) Structural basis for recognition of 2′,5′-linked oligoadenylates by human ribonuclease L. *EMBO J.*, **23**, 3929–3938.
41. Malathi,K., Dong,B., Gale,M. Jr and Silverman,R.H. (2007) Small self-RNA generated by RNase L amplifies antiviral innate immunity. *Nature*, **448**, 816–819.